This is an open access article published under a Creative Commons Attribution (CC-BY) License, which permits unrestricted use, distribution and reproduction in any medium, provided the author and source are cited.

Environmental Science & Technology

Article

Cite This: Environ. Sci. Technol. 2018, 52, 152−161

pubs.acs.org/est

Sustained Bauxite Residue Rehabilitation with Gypsum and Organic Matter 16 years after Initial Treatment

Andrew W. Bray,*[,†] Douglas I. Stewart,[‡] Ronan Courtney,[§] Simon P. Rout,[∥] Paul N. Humphreys,[∥] William M. Mayes,[⊥] and Ian T. Burke[†]

[†]School of Earth and Environment, University of Leeds, Leeds LS2 9JT, U.K.

[‡]School of Civil Engineering, University of Leeds, Leeds LS2 9JT, U.K.

[§]Department of Biological Sciences & The Bernal Institute, University of Limerick, Limerick, Ireland

[∥]Department of Chemical and Biological Sciences, University of Huddersfield, Huddersfield HD1 3DH, U.K.

[⊥]School of Environmental Sciences, University of Hull, Hull HU6 7RX, U.K.

Supporting Information

ABSTRACT: Bauxite residue is a high volume byproduct of alumina manufacture which is commonly disposed of in purpose-built bauxite residue disposal areas (BRDAs). Natural waters interacting with bauxite residue are characteristically highly alkaline, and have elevated concentrations of Na, Al, and other trace metals. Rehabilitation of BRDAs is therefore often costly and resource/infrastructure intensive. Data is presented from three neighboring plots of bauxite residue that was deposited 20 years ago. One plot was amended 16 years ago with process sand, organic matter, gypsum, and seeded (fully treated), another plot was amended 16 years ago with process sand, organic matter, and seeded (partially treated), and a third plot was left untreated. These surface treatments lower alkalinity and salinity, and thus produce a substrate more suitable for biological colonisation from seeding. The reduction of pH leads to much lower Al, V, and As mobility in the actively treated residue and the beneficial effects of treatment extend passively 20−30 cm below the depth of the original amendment. These positive rehabilitation effects are maintained after 2 decades due to the presence of an active and resilient biological community. This treatment may provide a lower cost solution to BRDA end of use closure plans and orphaned BRDA rehabilitation.

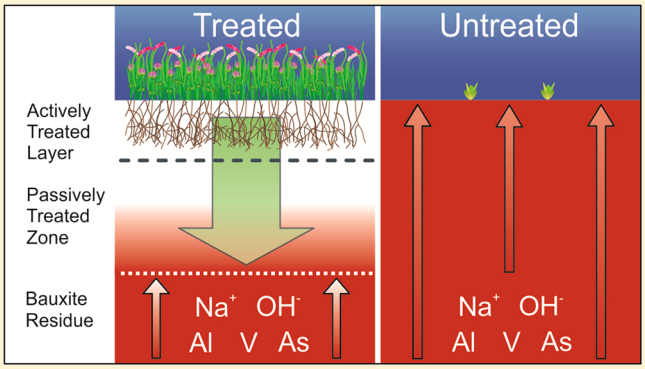

INTRODUCTION

Globally, > 100 million tonnes of alumina is produced annually.[1] Producing 1 tonne of alumina generates 1−2 tonnes of bauxite residue (known as "red mud"). The residue varies with ore type, but all are alkaline, sodic, and contain similar minerals. In the Bayer process bauxite ore is digested with NaOH at high temperature and pressure which results in recrystallization of iron oxides present. Silica is a common impurity, which is removed from solution by precipitation of a range of characteristic Na- and Ca-aluminosillicate phases (e.g., sodalite and cancrinite).[2,3] These "desilication products" reside predominantly in the fine fraction. Residual aluminum (oxy)hydroxide phases, quartz, zircon and titanium oxides (e.g., rutile and perovskite) also occur in the residues.[2,3]

Bauxite residue has few uses (cement, iron and steel production, construction materials) and most is sent to bauxite residue disposal areas (BRDAs).[4] The liquid from bauxite residue is very alkaline (pH 11−13) and contains abundant sodium.[5−7] Subsequent dissolution of desilication products such as sodalite (eq 1.) and cancrinite (eq 2), along with associated amorphous secondary phases, generates further alkalinity and releases sodium in the long term.[8−10] Trace elements in bauxite, such as V and As, become concentrated in the residue, and are often hosted in surface complexes and secondary phases.[10−14] This can be environmentally problematic as Al, V, and As form aqueous oxyanions in alkaline conditions which sorb poorly to sediments.[15,16]

$$Na_6(Al_6Si_6O_{24}).2NaOH + 24H_2O \leftrightarrow 8Na^+ + 8OH^- + 6Al(OH)_3 + 6H_4SiO_4 \quad (1)$$

$$Na_6(Al_6Si_6O_{24}).2CaCO_3 + 26H_2O \leftrightarrow 6Na^+ + 2Ca^{+2} + 8OH^- + 2HCO_3^- + 6Al(OH)_3 + 6H_4SiO_4 \quad (2)$$

Received: July 13, 2017
Revised: November 17, 2017
Accepted: November 28, 2017
Published: November 28, 2017

 © 2017 American Chemical Society

DOI: 10.1021/acs.est.7b03568
Environ. Sci. Technol. 2018, 52, 152−161

When left untreated, bauxite residue is infiltrated by CO_2 and the formation of aqueous and solid carbonate consumes OH^-, lowering pH.[17−19] The depth to which this process can act within bauxite residue is controlled by the rate of in-gassing and diffusion of CO_2. These process can be enhanced by gypsum addition, providing excess Ca^{2+} for precipitation of carbonate.[20] These reactions occur rapidly at high pH and can eventually buffer the pH to 7.5−8.5.[17,21] Previous work has shown that gypsum addition can also decrease the mobility of trace metals and Al in bauxite residue effected soils.[17,21] Other approaches to decrease bauxite residue salinity and alkalinity, such as treatment with acid[22] and seawater,[23] tend to only neutralize the aqueous, not the solid alkalinity generating phases. Ion exchange resins,[24] and bipolar-membranes electrodialysis[25] have been used to increase the longevity of treatment, yet these approaches rely on continued management and the utilization of products by an active refinery. As such, common end-of-use practice is to cap BRDAs with an impermeable layer, cover with topsoil, and revegetate. The costs "cap and cover" approaches are high (e.g., 100k €/ha has been estimated for the BRDA in this study). However, abandoning BRDAs without surface cover may lead to problems with long-term water infiltration and dust formation.

Over the last 15 years Courtney and others have examined the effect of coarse fraction bauxite residue (process sand), gypsum, and organic matter on the revegetation of bauxite residue in a BRDA.[26−36] These studies have assessed site rehabilitation by investigating macro- and microbiology, nutrient availability, and the chemical nature of the substrate. Beneficial effects from biorehabilitation have also been reported elsewhere.[37,38] Yet, little is known of the longevity and reliability of such surface treatments. Lack of long-term data, and poorly constrained audit trails regarding treatment and planting histories, can limit their viability in BRDA closure plans. The objective of this study was to assess the long-term effects of a surface treatment to bauxite residue. Here we report the chemical and mineralogical data sampled from depth profiles of bauxite residue nearly two decades after initial treatment, and evaluate the ability of these treatments to provide sustained rehabilitation of the substrate and associated fluid.

MATERIALS AND METHODS

In September 2015 trial pits were dug to ∼60 cm in a BRDA located in a European Union member state with a temperate oceanic climate (average annual rainfall ∼1m). At this site bauxite residue was deposited into a 3 m deep disposal cell in 1995, and subsequently treated to encourage revegetation in 1999. Therefore, sampling was undertaken 20 years after deposition and 16 years after treatment.[31] Three plots within the BRDA were investigated. The fully treated plot was amended with gypsum (3% w/w rotavated-in to a depth 30 cm), process sand (10% w/w rotavated-in to a depth of 30 cm), spent mushroom compost (80t Ha^{1-} rotavated-in to a depth of 20 cm), and seeded with a grassland mix (*Agrostis stolonifera, Holcus lanatus, Lolium perenne, Trifolium repens,* and *Trifolium pratense*; 100 kg/ha).[31] The partially treated plot was amended only with process sand, spent mushroom compost, and then seeded. The third plot was left untreated. Samples of bauxite residue were collected to a depth of 50 cm from the trial pits in each of three different treatment zones. Duplicate sample profiles in each plot were taken from two separate clean vertical surfaces of trial pits and stored in polypropylene tubes. The dual depth profiles were sampled to observe and account for heterogeneity in the residue.

Field moist samples were stored at 5 °C before aqueous extraction for major and trace metals. Ten gram subsamples were mixed with 10 mL of ultrapure water (18.5 MΩ) and shaken at room temperature for 7 days. The solution pH was measured using a Thermo Scientific Orion ROSS Ultra electrode calibrated with 4.00, 7.00, and 10.00 buffers (Fisher Scientific). One gram field moist subsamples were mixed with 10 mL of a 0.1 M Na_2HPO_4 in 0.01 M NaOH and shaken at room temperature for 7 days for phosphate extraction of metal oxyanions. Supernatant solutions from both the water and phosphate extractions were filtered through 0.2 μm disposable poly(ether sulfone) filters (Sartorius) and acidified in 5% HNO_3 for subsequent aqueous analysis by ICP-OES (Thermo Fisher iCAP 7400 Radial ICP-OES) (see SI Section S1 for further details).

Further 10 g field moist subsamples were also dried at 105 °C for 24 h to determine residue water content and for subsequent analysis by X-ray ray diffraction (XRD; Bruker D8 Advance diffractometer, 12 min scans, 2 to 70° 2θ), X-ray fluorescence (XRF, Olympus Innovex X-5000 XRF analyzer) and total carbon analysis (TC; LECO SC-144DR carbon analyzer). The crystalline phases present were determined from XRD patterns by peak fitting using EVA (version 3.0, Bruker), and semiquantitative relative proportions were calculated by Rietveld refinement using Topas (version 4.2, Bruker). Total organic carbon (TOC) were measured after a 24 h digestion in 10% HCl at room temperature. Total inorganic carbon (TIC) was calculated from TC and TOC measurements.

Acid soluble inorganic and organic substances (AIC and AOC) were determined in 12 samples after extraction with 2 M HCl (1 g soil in 5 mL of 2 M HCl for 3 days at 4 °C). The extractant was then separated by centrifugation at 8000*g* for 10 min, pH neutralized by dropwise addition of 2 M NaOH, evaporated to dryness; and finally the resulting solid dissolved in ultrapure water at 1 $g{\cdot}L^{-1}$.[39] Total carbon and total inorganic carbon in the extractant was determined using a Shimadzu total organic carbon analyzer 5050A (LOD 4 $\mu g\ kg^{-1}$).

Separate samples of bauxite residue were collected from beneath the exposed vertical surface of each trial pit using a clean spatula, and sealed in sterile polypropylene centrifuge tubes. These samples for DNA analysis were refrigerated within 4 h and frozen within 48 h. DNA was isolated from 0.5 g of each sample using the MPBio FastDNA SPIN Kit for Soil. Isolated DNA mass from each sample was determined by Qubit dsDNA High Sensitivity assay on a Qubit Fluorometer (Life Technologies; further details of quantification are in SI Section S3). DNA samples were sent to the Centre for Genomic Research, University of Liverpool, where Illumina TruSeq adapters and indices were attached to DNA fragments in a two-step PCR amplification that targets the V4 hyper-variable region of the 16s rRNA gene,[40] and the result was sequenced on the MiSeq platform. Reads were processed using the UPARSE pipeline[41] within the USEARCH software package (version 10, SI Section S3).[42] Sequence reads were allocated to operationally taxonomic units (OTUs) based on a minimum sequence identity of 97% between the putative OTU members, and then classified using the SILVA Living Tree Project 16s database, version 123.[43]

Difference in average element concentration between plot treatments (untreated, fully treated, and partially treated) was tested by ANCOVA (Analysis of Co-Variance) using a general

DOI: 10.1021/acs.est.7b03568
Environ. Sci. Technol. 2018, 52, 152−161

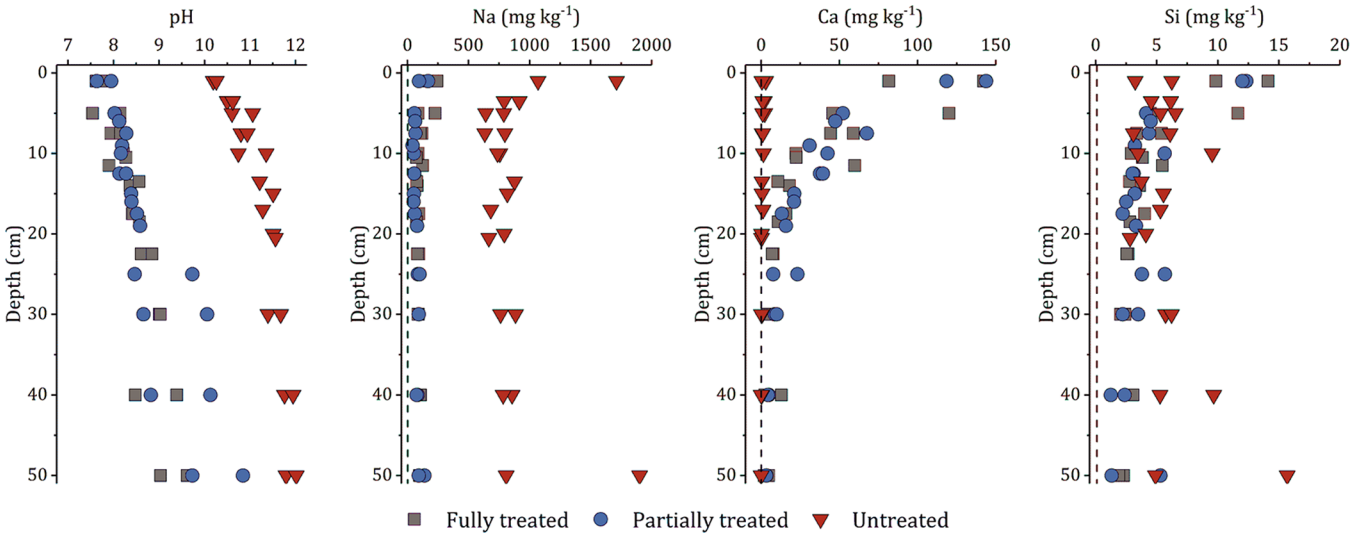

Figure 1. pH, Na, Si, and Ca aqueously extracted from fully treated, partially treated, and untreated bauxite residue as a function of depth. The dotted line represents the limit of detection for element.

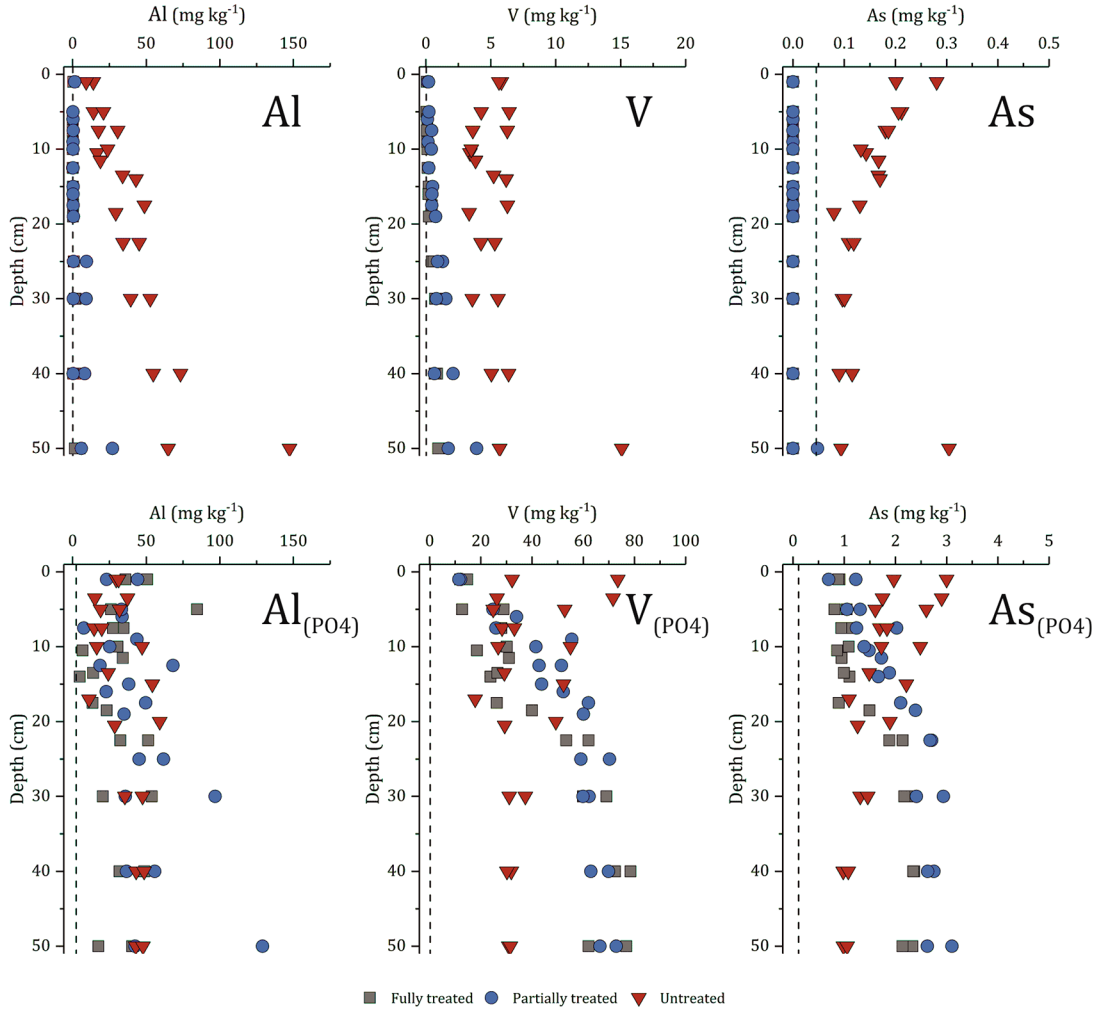

Figure 2. Concentrations of Al, V, and As in solution following aqueous and phosphate (PO4) extractions from fully treated, partially treated, and untreated bauxite residue as a function of depth. Note the change in *x*-axis scale for aqueous and phosphate extracted V and As. The dotted line represents the limit of detection for each element.

linear model to assess difference in average concentrations across the treatments, with depth of sample as a covariate. Pairwise comparisons were tested by posthoc Tukey test using a significance level of $p = 0.05$. Statistical significance was

DOI: 10.1021/acs.est.7b03568
Environ. Sci. Technol. 2018, 52, 152−161

Table 1. Semi-Quantitative Percentage of Crystalline Phases Present in Bauxite Residue As a Function of Treatment and Average Across Depth, Fitted Using Rietveld Refinement[a]

	Fe oxyhydroxides		Al oxyhydroxides			desilication products		Ti oxides	
	goethite	hematite	gibbsite	boehmite	katoite	cancrinite	sodalite	perovskite	
treatment site	α-FeO(OH)	Fe_2O_3	$Al(OH)_3$	γ-AlO(OH)	$Ca_3Al_2(OH)_{12}$	$Na_6Ca_2Al_6Si_6O_{24}(CO_3)_2$	$Na_8Al_6Si_6O_{24}(OH)_2$	$CaTiO_3$	other minerals
	%	%	%	%	%	%	%	%	%
untreated	21	16	8	10	2	14	1	20	9
fully treated	24	19	8	7	3	10	<0.5	20	9
partially treated	19	16	11	10	10	10	<0.5	15	8

[a]Uncertainty on the Rietveld refinement is approximately 5%. Full details are available in SI Table S2.

expressed at $p < 0.05$ and $p < 0.001$ and the degrees of freedom for all tests varied between 19 and 64.

RESULTS

Sampling Observations. Both the fully treated and partially treated sites were vegetated with a variety of perennial grasses (*Holcus lanatus*), trifoliate clovers (*Trifolium pratense*), and occasional small shrubs (*Salix* spp.; SI Figure S1), as has been described previously.[31] The untreated plot was largely unvegetated with one or two areas of stunted grasses (SI Figure S1). The root zone of the fully treated and partially treated sites extended approximately 15 cm beneath the surface, and below 20 cm the substrate had the appearance of dewatered bauxite residue with little change in appearance to 50 cm depth. The untreated profile had no root zone and at all depths had a very similar appearance to the residue in the other profiles at depths below 20 cm. The bottom of the untreated pit filled with leachate to a depth of about 10 cm after 2 h.

Substrate Characteristics. The pH of the untreated residue was 10.2 at the surface and steadily increased to 12.0 at a depth of 50 cm (Figure 1; SI Table S2). The pH of the treated plots were notably and significantly lower ($p < 0.001$; SI Table S3). The fully treated residue was pH 7.6 at the surface, and increased steadily to a value of 9.6 at a depth of 50 cm. The pH value of the partially treated residue was 7.6 at the surface, increased steadily to a value of 10.8 at a depth of 50 cm, and was not significantly different from the fully treated residue ($p > 0.05$; Figure 1; SI Tables S2 and S3).

The amount of sodium available to aqueous extraction of the untreated bauxite residue was ~900 mg kg^{-1} of bauxite residue, and with exception of concentrations at the surface and at 50 cm there was little variation with depth (Figure 1, SI Table S2). The amount of Na that could be extracted from the fully treated and partially treated samples demonstrated no trend with depth and concentrations were not significantly different from each other ($p > 0.05$; SI Table S3). Fully and partially treated residue contained concentrations approximately 10−15% of those extracted from the untreated residue at the same depth ($p < 0.001$; Figure 1; SI Tables S2 and S3). The concentration of silicon available to aqueous extraction in the untreated bauxite residue was 5 mg kg^{-1}, and apart from the measured concentration from 50 cm there was minimal variation with depth (Figure 1, SI Table S2). Si concentrations extracted from fully treated and partially treated bauxite residue were ~4 mg kg^{-1} below 5 cm, and ~13 mg kg^{-1} above 5 cm, there was no significant difference between fully, partially, or untreated residue ($p > 0.05$; Figure 1; SI Tables S2 and S3). Calcium concentrations from the aqueous extraction of untreated bauxite residue ranged from 3 mg kg^{-1} at the surface to below the limit of detection at 50 cm (0.11 mg kg^{-1}) (Figure 1, SI Table S2). In contrast Ca concentrations from fully treated and partially treated samples were significantly different to the untreated residue ($p < 0.001$; SI Table S3), 143 mg kg^{-1} at the surface decreasing to ~10 mg kg^{-1} at 20 cm, with further slight concentration decrease to ~2 mg kg^{-1} at 50 cm with no significant difference between treatments ($p > 0.005$; Figure 1; SI Table S2−3).

The aluminum concentration available to aqueous extraction in untreated bauxite residue was ~10 mg kg^{-1} at the surface which increases steadily with depth to ~65 mg kg^{-1} at 50 cm (Figure 2. SI Table S2). Conversely, Al concentrations available in fully and partially treated samples were significantly different ($p < 0.001$, SI Table S3) and near the detection limit (0.09 mg kg^{-1}) at all depths, apart from at 30−50 cm where Al concentrations were 1−10 mg kg^{-1} (Figure 2. SI Table S2). There was no significant difference between treatments ($p > 0.05$, SI Table S3). The amount of vanadium available to aqueous extraction from untreated bauxite residue was ~5 mg kg^{-1} and did not vary greatly with depth (Figure 2. SI Table S2). Aqueous extractable V in fully treated and partially treated samples were near detection limit at the surface (0.03 mg kg^{-1}) and increased gradually with depth to maximum concentrations of 3.9 mg kg^{-1} at 50 cm, significantly different from untreated residue ($p < 0.001$, SI Table S3) but not significantly different between fully and partially treated residue ($p > 0.05$; Figure 2; SI Tables S2 and S3). Aqueous available arsenic concentrations from untreated bauxite residue were highest at the surface (0.3 mg kg^{-1}) and decrease with depth to 0.9 mg kg^{-1} at 50 cm depth (Figure 2. SI Table S2). With the exception of one sample, all measurements of aqueous extractable As from fully treated and partially treated bauxite residue were below detection limit (0.045 mg kg^{-1}) and significantly different from the untreated residue ($p < 0.001$; Figure 2; SI Tables S2 and S3). Extraction at high pH using disodium phosphate demonstrated substantial concentrations of Al, V, and As were available in all bauxite residue treatments. Phosphate extractable Al concentrations from all treatments are generally all 25−50 mg kg^{-1} at all depths (no significant differences between treatments; $p > 0.05$; SI Tables S2 and S3). V concentrations from the phosphate extraction of untreated bauxite residue range from 30 to 75 mg kg^{-1} at the surface to 30 mg kg^{-1} at 50 cm depth (Figure 2. SI Table S2). Phosphate available V from fully treated and partially treated samples was lowest at the surface (~15 mg kg^{-1}) and increases with depth to ~75 mg kg^{-1} at 50 cm, but with no significant differences between untreated, fully treated, or partially treated residue ($p > 0.05$; Figure 2. SI Table S2−3). Arsenic concentrations extracted from untreated bauxite residue at high pH with phosphate are

DOI: 10.1021/acs.est.7b03568
Environ. Sci. Technol. 2018, 52, 152−161

~2.5 mg kg^{-1} at the surface and decrease to <1 mg kg^{-1} at 50 cm (Figure 2. SI Table S2). Phosphate extractable As from fully treated and partially treated samples increase with depth from ~1 mg kg^{-1} at the surface to ~2.5 mg kg^{-1} at 50 cm (Figure 2. SI Table S2). Phosphate extractable As from fully treated and partially treated residue were significantly different ($p < 0.05$), though neither were significantly different from the untreated residue ($p > 0.05$; SI Table S3).

The water content of the residue (weight of water as % of dry weight) at both the fully and partially treated sites was over 50% near the surface, exhibited a minimum of ~30% at approximately 10 cm, and then increased to between 35 and 45% at depths below 20 cm (SI Table S2). In contrast the water content in the untreated profile was 35% near to the surface, exhibited a maximum value of ~50% at 10 cm, and then decreased slightly to 40% at depths below 30 cm. Water in the untreated residue was significantly different to fully treated residue ($p < 0.001$), but not significantly different from partially treated residue ($p > 0.05$; SI Table S3)

The bulk mineralogy of bauxite residue from all plots were largely similar and consist of 40−45% iron oxy-hydroxides, 20−30% aluminum oxy-hydroxides, 20−30% titanium oxides, and 10−15% feldspathoids (Table 1, SI Table S4). At the untreated bauxite residue plot there were no differences in the relative proportions of each phase with depth. Variations in the relative proportions of phases within the residue as a function of depth and treatment were within the range of uncertainty of Rietveld refinement (5%). The alkali generating feldspathoid and desilication product cancrinite was present at all depths in all treatment sites (Table 1, SI Table S4). There was little difference in the bulk elemental composition measured by XRF with either depth or treatment (SI Table S5). Fe, Al, Ca, Si, and Ti were the most abundant oxides in present each site (36 ± 3, 10 ± 2, 15 ± 2, 5 ± 1, and 4 ± 1 wt % respectively). Carbon was most concentrated in the top 10 cm of the fully treated profile (Figure 3), where TOC was approximately 2.5% and TIC was 1.5%. Below 10 cm there was no discernible difference in carbon content between the fully treated and untreated profiles. Samples of untreated bauxite had less than 0.5% TOC and TIC at all depths. Acid extractable inorganic carbon (AIC) and organic carbon (AOC) was only detectable in the top 10 cm of the fully treated and untreated bauxite residue, and was below or at the limit of detection (<4 μg kg^{-1}) in all other samples (SI Table S2).

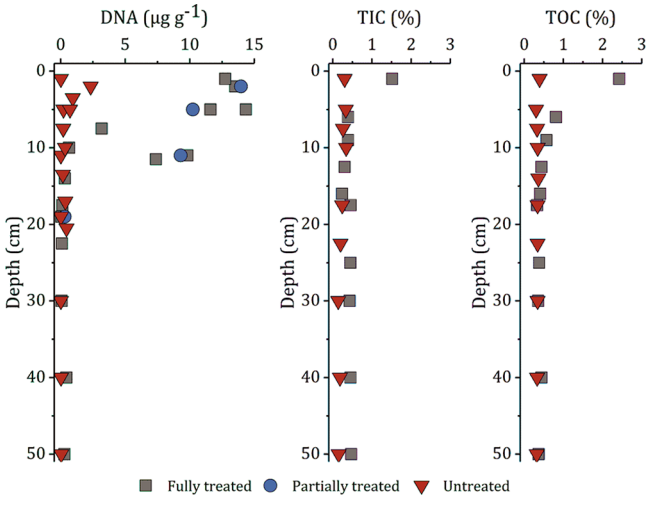

Figure 3. DNA, total inorganic carbon (TIC), and total organic carbon (TOC) concentrations in fully treated, partially treated, and untreated bauxite residue as a function of depth.

DNA mass isolated per gram of sample demonstrated a strong vertical gradient and significant difference between the treated (fully treated and partially treated) and untreated sites (Figure 3, SI Table S6). DNA was concentrated in the top 12 cm of the fully treated and partially treated sites where maximum concentrations were up to 14.3 μg g^{-1}. The highest concentration of DNA in the untreated samples was 2.3 μg g^{-1} in the near surface. Below 12 cm the DNA concentrations in the fully treated, partially treated and untreated residue were negligible.

Sufficient bacterial DNA was recovered from the fully treated substrate (2 cm), and partially treated substrate (2 and 5 cm) for Next Generation Sequencing (DNA recovery from the untreated substrate was insufficient). Nine phyla individually represented more the 1% of the population of each sample (SI Figure S2, Table S7). At this taxonomic level, there was little difference between bacterial communities of the fully treated and partially treated substrate, with the most abundant phyla being Acidobacteria (37% of reads), Actinobacteria (19%), Proteobacteria (18%), and Planctomycetes (14%). The most abundant class within the Acidobacteria phylum was Acidobacteria Gp6 (48% of Acidobacteria). Actinomycetales (74%) was the most abundant order within the Actinobacteria phylum. Alphaproteobacteria (67%) was the most abundant class within the Proteobacteria. 100% of the Planctomycetes phylum mapped onto the Planctomycetaceae family.

The alpha diversity indices for each sample are shown in SI Table S8. Here we use Hill numbers[44,45] as robust bacterial diversity measures which account for the distortions of rare taxa.[44−47] D_0^{α}, the operational taxonomic unit (OTU) richness, ranges from ~1250 to 3850, however this diversity index is very sensitive to rare taxa, and takes no account of OTU relative abundance. Indices that give a measure of the number of common (D_1^{α}) and dominant OTUs (D_2^{α}; sI Table S8), converge across the samples, demonstrating similar diversity in the OTU populations. Common OTUs represent >79% of total sequence reads in each sample, and dominant OTUs accounted for 51−62% of total reads in each sample.

DISCUSSION

The Geochemistry of 20 Year Old Untreated Bauxite Residue. Fresh bauxite residue is highly alkaline (pH 10−13), highly sodic (abundant mobile Na), contains abundant solid phase alkalinity (e.g., desalination products; 2−51%) and can also can contain trace metals above threshold intervention levels.[10,12,26,27,48−52] The desilication products in fresh residue tend to have higher proportion of sodalite to cancrinite[10] however, with age sodalite can transform into cancrinite.[53] Initially the high pH and sodium content are due to remnant NaOH from the Bayer Process. Previous work has shown that repeated replacement of pore water decreases the mass of fresh bauxite residue but does not alter final pH, Na^+, $Al(OH)_4^-$, CO_3^{2-}, or OH^- concentrations[8] due to the dissolution desilication products, and associated amorphous phases (eqs 1 and 2). When left untreated, the pH of bauxite residue is controlled by the balance between CO_2 infiltration from the atmosphere, and OH^- production through desilication product dissolution.

Twenty years after deposition, the measured pH of the untreated bauxite residue ranges from pH 10 at the surface to

DOI: 10.1021/acs.est.7b03568
Environ. Sci. Technol. 2018, 52, 152−161

pH 12 at 50 cm. XRD analysis indicates that cancrinite was the primary desilication product present (SI Table S4). At the surface, CO_2 in-gassing, in combination with cancrinite dissolution, and associated amorphous Fe, Al, and Si phase solubility, buffers the pore fluids to approximately pH 10. Atmospheric CO_2 in-gassing appears to extend ~20 cm from the surface (Figure 1). Below 20 cm the bauxite residue appears to be isolated from the atmosphere and dissolution of cancrinite results in higher pH (≥11.5; Figure 1). Cancrinite dissolution also controls long-term Na availability (eq 2), and results in aqueous available Na concentrations of ~900 mg kg^{-1} in untreated bauxite residue after 20 years. However, dissolution of cancrinite appears to be incongruent at high pH. Cancrinite dissolution should produce equimolar concentrations of Na, Si, and Al, (eq 2) but the measured concentrations are far from stoichiometric (SI Figure S3). Aqueous extractable Na concentrations from untreated samples are 100−400 times higher in concentration than extractable Si and 10−150 times the Al concentration, indicating a preferential retention of Si and Al in the solid phase.

This preferential retention of Al and Si in the solid phase is probably controlled by the precipitation of amorphous and crystalline secondary phases. At the highest pH measured, Al concentrations are close to equilibrium with gibbsite ($Al(OH)_3$) (SI Figure S3). The measured Al concentrations decrease as the pH decreases from 12 to 10, but exceeds concentrations in equilibrium with gibbsite. Over this pH range, Si concentrations are much lower than those expected for $SiO_{2(am)}$ equilibrium, suggesting an alternative solubility limiting phase. At high pH, with high Na concentrations, Al and Si can coprecipitate in amorphous cation-bridged aluminosilicate gels,[54] which may explain the low concentrations observed.

Sustained alkalinity generation throughout untreated bauxite residue is a concern because it may be associated with increased mobility of potentially toxic metal(oid) oxyanions such as Al, V, and As. Both V and As are reported to be present in bauxite residues primarily in the 5+ oxidation state as vanadate and arsenate species,[10,12] and are found as surface adsorbed species (V can also be associated with neoformed hydrogarnet phases such as Katoite).[12] Conversely, Al availability is usually controlled by the solubility of Al (oxy)hydroxide phases, which typically have much higher solubility at high pH (see Discussion above).[55] In alkaline phosphate extractions both OH^- and phosphate ions compete strongly for available sorption sites and promote the mobility of metal oxyanions.[14,20] The results of these extractions, therefore, demonstrate that there is abundant V and As adsorbed to bauxite residue (Figure 2). In the untreated samples, where pH > 10, As and V sorb poorly to mineral surfaces,[14−16,21,56−58] which is why only 10 and 15% of the phosphate extractable As and V respectively were extractable water this fraction will be mobile in residue pore waters.

In summary, the bauxite residue from the untreated plot retains many of the characteristics of the fresh bauxite residue 20 years after deposition: high pH, a sizable quantity of desilication products (particularly cancrinite), abundant available Na, high Al, V, and As concentrations, low organic carbon concentrations. Thus, untreated, it is an environment that is not conducive to spontaneous macro- or microorganism colonization through translocation.

Treated Bauxite Residue. Sixteen years after bauxite residue treatment with process sand, organic matter and gypsum, significant pH reduction (2 units) was observed over a depth that extends at least 30 cm below the actively treated surface layer (Figure 1; SI Table S2). Aqueous sodium concentrations were an order of magnitude lower in the treated plots than untreated plot at all depths (Figure 1; SI Table S2), and the availability of aluminum, vanadium, and arsenic were all lower in treated than untreated bauxite residue (Figure 2; SI Table S2). These observations demonstrate that positive treatment effects observed in the short term are sustained, such as improved permeability, particle aggregation, and drainage; pH neutralization; decreased Na, Al, and Fe availability.[28,29] In natural soils, organic matter plays a key role in controlling particle aggregation,[59−61] and the application of spent mushroom compost may have improved residue structure. In highly alkaline conditions, organic matter dissolves and hydrolyses to form humic substances and lower molecular weight organic anions.[62−64] This process lowers pH and releases organic bound nutrients to the local environment. Other studies have reported significant reduction in pH following organic matter application to bauxite residue.[28,29,65,66]

Gypsum application enhances pH neutralization by CO_2 in-gassing via the precipitation of $CaCO_3$.[20,21] The net reaction for this mechanism is

$$CaSO_4.2H_2O + 2OH^- + CO_2 \rightleftharpoons CaCO_3 + SO_4^{2-} + 3H_2O \quad (3)$$

Increased CO_2 in-gassing and formation of dissolved carbonate species (SI eqs S2−7) can buffer the pH to 7.5−8, similar to natural alkaline soils, thus producing an environment less hostile to biological colonisation. At this site bauxite residue treatment with gypsum (in addition to process sand and organic matter) resulted in greater plant biomass in the first two years of growth,[26−28] and a more diverse and developed vegetation succession after 6 years (i.e., partial replacement of clover by more extensive grass cover and the establishment of small shrubs).[31] However, 16 years after treatment, there is no significant chemical or microbiological difference between the fully and partially treated substrate.

Long-term alkalinity generation and sodium release in the 20 year old bauxite residue is controlled by cancrinite dissolution. Cancrinite dissolution kinetics as a function of pH is unreported in the literature, but the feldspathoids leucite and nepheline exhibit dissolution kinetics that decrease by an order of magnitude as pH decreases from 12 to 7.[67−70] The dissolution kinetics of multioxide silicates, including aluminosilicates, are controlled by the solubilities of secondary phases,[71] thus it is inferred that these decreases in feldspathoid dissolution rate are linked to the solubilities of secondary aluminum and silicon phases. It is reasonable to expect cancrinite dissolution kinetics to vary with pH in a similar manner to other feldspathoids, decreasing by an order of magnitude between pH 12 and 7. This suggests pH conditions established in treated bauxite residue from organic matter and gypsum addition decrease the rate of OH^- and Na^+ production from the dissolution of cancrinite and associated secondary phases (Figure 1).

Aqueous extracted aluminum concentrations from partially and fully treated bauxite residue plotted as a function of pH (SI Figure S3) fall on a line parallel to, but in between, the solubility lines of gibbsite and $Al(OH)_{3\ (am)}$. This is different to the trend observed for the untreated samples at higher pH, suggesting a different solubility controlling phase. Between pH 8 and 10 formation of Dawsonite ($NaAlCO_3(OH)_2$) and an

DOI: 10.1021/acs.est.7b03568
Environ. Sci. Technol. 2018, 52, 152−161

amorphous precursor to boehmite have been observed in bauxite residue treatment.[12,72] and may be the solubility controlling phases at this site. The phosphate extraction shows that there is abundant extractable Al, V, and As in both the partially and fully treated bauxite residue (Figure 2; SI Table S2). However, the aqueous extractions showed that nearer to neutral pH Al is secured in secondary phases, and the majority of V and As is sorbed to mineral surfaces[14−16,21,56−58] making Al, V, and As, much less available to aqueous solution (Figure 2).

Long-Term Maintenance of Beneficial Conditions. Rehabilitation of bauxite residue disposal areas by vegetation using the treatments described here is a pH dependent processes with benefits extending 20−30 cm beyond the initial treatment depth. After 20 years of rainwater infiltration the alkalinity generating phases have not been exhausted, thus other processes must be controlling residue neutralization. Sixteen years after treatment, the original additives are largely unobservable, with little chemical difference remaining from the application of gypsum. This suggests that the development of resilient vegetation on bauxite residue, along with associated rhizosphere microorganisms, may drive long-term stability and chemical safety of treated bauxite residue. The organic matter applied to the surface layers is only detected in small quantities (Figure 3) and has likely been degraded and recycled into plants and microorganisms. The products of gypsum addition are minimal; calcite was undetectable by XRD, and there is only a slight accumulation of Ca and TIC toward the surface of both treated zones. Process sand was present in the surface layer when sampling but heterogeneously distributed and undetectable mineralogically by XRD and chemically by XRF.

The supply of H^+ ions to depth, that is drives pH neutralization in treated bauxite residue, may be photosynthetic in origin. This can occur via a combination of three mechanisms: (a) enhanced CO_2 flux from plant root and associated microorganism respiration; (b) organic matter degradation in the biologically active surface layer, producing low molecular weight organic acids; and (c) secretion of low molecular weight organic acids by plant roots and rhizospheric microorganisms. The carbon flux from atmosphere to rhizosphere is well documented in both the short (i.e., respiration), and medium terms (organic matter production).[73] Quantification of extracted DNA from both the treated plots suggests a zone of greater biological activity in the top 12 cm of treated bauxite residue (Figure 3). DNA recovery is media dependent, with particle size and pH potentially affecting the efficiency of extraction. This uncertainty may over emphasize the gradient of biological activity with depth, and between treated and untreated samples. The extracted DNA concentrations from the top 12 cm of treated bauxite residue are within the range of extracted DNA concentrations from natural soils (very approximate soil DNA concentrations range from 2.5 to 26.9 $\mu g\ g^{-1}$).[74] DNA recovery from this site's untreated bauxite residue was insufficient for Next-Generation Sequencing, however other workers have shown bauxite residue to contain alkali tolerant bacteria.[75] Sequenced DNA recovered from the root zone substrate of the fully and partially treated bauxite residue was dominated by the phyla Acidobacteria, Actinobacteria, Proteobacteria, and Planctomycetes. Natural soil root zone or rhizosphere bacterial communities frequently contain Actinobacteria, Bacteroidetes, Firmicutes, and Proteobacteria taxa,[76−78] which, with the exception of Firmicutes, are present in our treated bauxite residue (SI Figure S2, Table S7). Many taxa of Acidobacteria are known to be tolerant to high pH, and show increasing relative abundance with increasing pH from 5.5 pH.[79−82] Many Planctomycetes taxa are halotolerant,[83−87] existing in freshwater, marine, and brackish environments. The presence of these phyla suggests the microbial communities in the fully and partially treated bauxite residue are in transition between a highly alkaline and saline residue microbiome, and a plant supported subsurface microbiome.

Surface treatment with process sand, gypsum, and organic matter is a stable, reliable, and safe solution to bauxite residue rehabilitation. Bauxite residue pH is neutralized, Na^+ is less available, and metal oxyanions (Al, V, and As) are less mobile. The beneficial effects of treatment are long-term and extend 20−30 cm beyond the depth of application. The formation a passively treated zone, which is ≥20% of the total disposal cell depth, is sufficient to separate the surface environments from the potentially highly alkaline, sodium rich, and trace metal containing residue at depth. The presence of alkalinity generating phases in both treated plots highlights the importance of maintaining a strong biologically active surface layer. Were this layer to be removed or substantially disrupted, and its supply of acid neutralizing molecules lost, the system would likely return to a high pH steady state, with high Na, Al, V, and As concentrations, similar to those observed in the untreated bauxite residue.

This is the first observation of a shallow surface layer of actively treated and vegetated residue producing passive positive rehabilitation effects into deeper layers. This rehabilitation is likely driven by biology activity at the surface and continues long after the original treatment constitutes (gypsum, organic matter) have been depleted. Rehabilitation has resulted in a physical separation between deeper zones within the residue (potentially containing high alkalinity, sodium, and trace metals) and the bottom of the rooted zone at around 20 cm. Rehabilitation decreases the likelihood of plants being exposed to the negative characteristics of bauxite residue, and lowers the possibility of trace metal transfer into foliage and the wider ecosystem. The benefits of this surface treatment extend beyond the environmental; the cost of application is approximately 10k €/ha, whereas the cap and coverestimate for this BRDA is 100k €/ha. Gypsum application accounts for approximately 50−70% of the total treatment cost, and assessment of its value for long-term rehabilitation is important. Our results suggest the development of a healthy vegetation cover is key to long-term stability of residue rehabilitation and previous work has demonstrated the role of gypsum in rapidly, and successfully establishing a resilient vegetation layer.[26−28,31,32,35] Gypsum application may, therefore, offer additional security in vegetation establishment, and the ultimate success and longevity of rehabilitation. However, 16 years after application there are no significant chemical benefits from gypsum addition. Our study demonstrates surface amendment of this nature is a viable closure option for active BRDAs and a particularly good choice for rehabilitation of orphan sites where there is an acute need to protect the public and environment at the lowest possible costs.

■ ASSOCIATED CONTENT

Supporting Information

The Supporting Information is available free of charge on the ACS Publications website at DOI: 10.1021/acs.est.7b03568.

DOI: 10.1021/acs.est.7b03568
Environ. Sci. Technol. 2018, 52, 152−161

Detailed aqueous analysis, DNA extraction, quantification, and post sequence processing methods. Stepwise reactions of gypsum promoted $CaCO_3$ precipitation and pH neutralization. On site photographs of the trial pits. Additional figures of bacterial community composition and elemental ratios and solubility. Additional tables with full analytical results. Sequence reads have been uploaded to the National Center for Biotechnology Information (NCBI) under the Sequence Read Archive (SRA) accession PRJNA419106. Collectively, the paper and these sources provide all the relevant data for this study (PDF)

AUTHOR INFORMATION

Corresponding Author

*E-mail: a.w.bray@leeds.ac.uk.

ORCID

Andrew W. Bray: 0000-0001-5399-6647

Ian T. Burke: 0000-0002-0484-568X

Notes

The authors declare no competing financial interest.

ACKNOWLEDGMENTS

This research was funded by grant NE/L01405X/1 as part of the Resource Recovery from Waste programme administered by the Natural Environment Research Council (NERC), UK. The authors would like to thank Andy Connelly, Lesley Neve, Stephen Reid, Sheena Bennett, and David Elliott at the University of Leeds for technical support.

REFERENCES

(1) World Aluminium. World Aluminium — Alumina Production http://www.world-aluminium.org/statistics/alumina-production/ (accessed May 26, 2017).

(2) Snars, K.; Gilkes, R. J. Evaluation of bauxite residues (red muds) of different origins for environmental applications. *Appl. Clay Sci.* **2009**, *46* (1), 13−20.

(3) International Aluminium Institute. *Bauxite Residue Management: Best Practice* www.european-aluminium; 2015.

(4) Power, G.; Gräfe, M.; Klauber, C. Bauxite residue issues: I. Current management, disposal and storage practices. *Hydrometallurgy* **2011**, *108* (1), 33−45.

(5) Hind, A. R.; Bhargava, S. K.; Grocott, S. C. The surface chemistry of Bayer process solids: a review. *Colloids Surf., A* **1999**, *146* (1), 359−374.

(6) Czop, M.; Motyka, J.; Sracek, O.; Szuwarzyński, M. Geochemistry of the Hyperalkaline Gorka Pit Lake (pH>13) in the Chrzanow Region, Southern Poland. *Water, Air, Soil Pollut.* **2011**, *214* (1−4), 423−434.

(7) Mayes, W. M.; Jarvis, A. P.; Burke, I. T.; Walton, M.; Feigl, V.; Klebercz, O.; Gruiz, K. Dispersal and Attenuation of Trace Contaminants Downstream of the Ajka Bauxite Residue (Red Mud) Depository Failure, Hungary. *Environ. Sci. Technol.* **2011**, *45* (12), 5147−5155.

(8) Thornber, M.; Binet, D. Caustic Soda Adsorption on Bayer Residues. In *5th International Alumina Quality Workshop*; AQW Inc., Bunbury, 1999; pp 498−507.

(9) Menzies, N. W.; Fulton, I. M.; Kopittke, R. A.; Kopittke, P. M. Fresh Water Leaching of Alkaline Bauxite Residue after Sea Water Neutralization. *J. Environ. Qual.* **2009**, *38* (5), 2050.

(10) Gräfe, M.; Power, G.; Klauber, C. Bauxite residue issues: III. Alkalinity and associated chemistry. *Hydrometallurgy* **2011**, *108* (1), 60−79.

(11) Brunori, C.; Cremisini, C.; Massanisso, P.; Pinto, V.; Torricelli, L. Reuse of a treated red mud bauxite waste: studies on environmental compatibility. *J. Hazard. Mater.* **2005**, *117* (1), 55−63.

(12) Burke, I. T.; Mayes, W. M.; Peacock, C. L.; Brown, A. P.; Jarvis, A. P.; Gruiz, K. Speciation of arsenic, chromium, and vanadium in red mud samples from the Ajka spill site, Hungary. *Environ. Sci. Technol.* **2012**, *46*, 3085−3092.

(13) Klebercz, O.; Mayes, W. M.; Anton, Á. D.; Feigl, V.; Jarvis, A. P.; Gruiz, K.; Mander, Ü.; Csákberényi-Malasics, D.; Tóth, Á.; Czitrovsky, A.; et al. Ecotoxicity of fluvial sediments downstream of the Ajka red mud spill, Hungary. *J. Environ. Monit.* **2012**, *14* (8), 2063.

(14) Lockwood, C. L.; Mortimer, R. J. G.; Stewart, D. I.; Mayes, W. M.; Peacock, C. L.; Polya, D. A.; Lythgoe, P. R.; Lehoux, A. P.; Gruiz, K.; Burke, I. T. Mobilisation of arsenic from bauxite residue (red mud) affected soils: Effect of pH and redox conditions. *Appl. Geochem.* **2014**, *51*, 268−277.

(15) Peacock, C. L.; Sherman, D. M. Vanadium(V) adsorption onto goethite (α-FeOOH) at pH 1.5 to 12: a surface complexation model based on ab initio molecular geometries and EXAFS spectroscopy. *Geochim. Cosmochim. Acta* **2004**, *68* (8), 1723−1733.

(16) Mamindy-Pajany, Y.; Hurel, C.; Marmier, N.; Roméo, M. Arsenic adsorption onto hematite and goethite. *C. R. Chim.* **2009**, *12* (8), 876−881.

(17) Renforth, P.; Mayes, W. M.; Jarvis, A. P.; Burke, I. T.; Manning, D. A. C.; Gruiz, K. Contaminant mobility and carbon sequestration downstream of the Ajka (Hungary) red mud spill: The effects of gypsum dosing. *Sci. Total Environ.* **2012**, *421*, 253−259.

(18) Alcoa. *Pinjarra Refinery Long Term Residue Management Strategy*, 2011.

(19) Alcoa. *Kwinana Refinery Long Term Residue Management Strategy*, 2012.

(20) Burke, I. T.; Peacock, C. L.; Lockwood, C. L.; Stewart, D. I.; Mortimer, R. J. G.; Ward, M. B.; Renforth, P.; Gruiz, K.; Mayes, W. M. Behavior of Aluminum, Arsenic, and Vanadium during the Neutralization of Red Mud Leachate by HCl, Gypsum, or Seawater. *Environ. Sci. Technol.* **2013**, *47* (12), 6527−6535.

(21) Lehoux, A. P.; Lockwood, C. L.; Mayes, W. M.; Stewart, D. I.; Mortimer, R. J. G.; Gruiz, K.; Burke, I. T. Gypsum addition to soils contaminated by red mud: implications for aluminium, arsenic, molybdenum and vanadium solubility. *Environ. Geochem. Health* **2013**, *35* (5), 643−656.

(22) Kirwan, L. J.; Hartshorn, A.; McMonagle, J. B.; Fleming, L.; Funnell, D. Chemistry of bauxite residue neutralisation and aspects to implementation. *Int. J. Miner. Process.* **2013**, *119*, 40−50.

(23) Hanahan, C.; McConchie, D.; Pohl, J.; Creelman, R.; Clark, M.; Stocksiek, C. Chemistry of Seawater Neutralization of Bauxite Refinery Residues (Red Mud). *Environ. Eng. Sci.* **2004**, *21* (2), 125−138.

(24) Wightman, G.; Davy Mckee Limited. Process for the removal of sodium values from sodium contaminated solids. CA 2132638A1, 1994.

(25) Kishida, M.; Harato, T.; Tokoro, C.; Owada, S. In situ remediation of bauxite residue by sulfuric acid leaching and bipolar-membrane electrodialysis. *Hydrometallurgy* **2016**.1705810.1016/j.hydromet.2016.04.012

(26) Courtney, R.; Timpson, J. P.; Grennan, E. Growth of Trifolium pratense in Red Mud Amended With Process Sand, Gypsum and Thermally Dried Sewage Sludge. *Int. J. Surf. Min., Reclam. Environ.* **2003**, *17* (4), 227−233.

(27) Courtney, R. G.; Timpson, J. P. Nutrient status of vegetation grown in alkaline bauxite processing residue amended with gypsum and thermally dried sewage sludge - A two year field study. *Plant Soil* **2004**, *266* (1−2), 187−194.

(28) Courtney, R. G.; Timpson, J. P. Reclamation of Fine Fraction Bauxite Processing Residue (Red Mud) Amended with Coarse Fraction Residue and Gypsum. *Water, Air, Soil Pollut.* **2005**, *164* (1−4), 91−102.

(29) Courtney, R. G.; Jordan, S. N.; Harrington, T. Physico-chemical changes in bauxite residue following application of spent mushroom compost and gypsum. *L. Degrad. Dev.* **2009**, *20* (5), 572−581.

DOI: 10.1021/acs.est.7b03568
Environ. Sci. Technol. 2018, 52, 152−161

(30) Courtney, R.; Mullen, G. Use of Germination and Seedling Performance Bioassays for Assessing Revegetation Strategies on Bauxite Residue. *Water, Air, Soil Pollut.* **2009**, *197* (1−4), 15−22.
(31) Courtney, R.; Mullen, G.; Harrington, T. An evaluation of revegetation success on bauxite residue. *Restor. Ecol.* **2009**, *17* (3), 350−358.
(32) Courtney, R.; Harrington, T. Growth and nutrition of Holcus lanatus in bauxite residue amended with combinations of spent mushroom compost and gypsum. *L. Degrad. Dev.* **2012**, *23* (2), 144−149.
(33) Courtney, R.; Kirwan, L. Gypsum amendment of alkaline bauxite residue − Plant available aluminium and implications for grassland restoration - ScienceDirect. *Ecol. Eng.* **2012**, *42*, 279−282.
(34) Schmalenberger, A.; O'Sullivan, O.; Gahan, J.; Cotter, P. D.; Courtney, R. Bacterial Communities Established in Bauxite Residues with Different Restoration Histories. *Environ. Sci. Technol.* **2013**, *47* (13), 7110−7119.
(35) Courtney, R.; Feeney, E.; O'Grady, A. An ecological assessment of rehabilitated bauxite residue. *Ecol. Eng.* **2014**, *73*, 373−379.
(36) Courtney, R.; Harris, J. A.; Pawlett, M. Microbial Community Composition in a Rehabilitated Bauxite Residue Disposal Area: A Case Study for Improving Microbial Community Composition. *Restor. Ecol.* **2014**, *22* (6), 798−805.
(37) Santini, T. C.; Kerr, J. L.; Warren, L. A. Microbially-driven strategies for bioremediation of bauxite residue. *J. Hazard. Mater.* **2015**, *293*, 131−157.
(38) Zhu, F.; Li, X.; Xue, S.; Hartley, W.; Wu, C.; Han, F. Natural plant colonization improves the physical condition of bauxite residue over time. *Environ. Sci. Pollut. Res.* **2016**, *23* (22), 22897−22905.
(39) Eaton, A. D.; Clesceri, L. S.; Rice, E. W.; Greenberg, A. E. *Standard Methods for the Examination of Water & Wastewater*, 21st ed.; American Public Health Association: Washington, DC, 2005.
(40) Caporaso, J. G.; Lauber, C. L.; Walters, W. A.; Berg-Lyons, D.; Lozupone, C. A.; Turnbaugh, P. J.; Fierer, N.; Knight, R. Global patterns of 16S rRNA diversity at a depth of millions of sequences per sample. *Proc. Natl. Acad. Sci. U. S. A.* **2011**, *108 Suppl 1* (Supplement 1), 4516−4522.
(41) Edgar, R. C. UPARSE: highly accurate OTU sequences from microbial amplicon reads. *Nat. Methods* **2013**, *10* (10), 996−998.
(42) Edgar, R. C. Search and clustering orders of magnitude faster than BLAST. *Bioinformatics* **2010**, *26* (19), 2460−2461.
(43) Yarza, P.; Richter, M.; Peplies, J.; Euzeby, J.; Amann, R.; Schleifer, K.-H.; Ludwig, W.; Glöckner, F. O.; Rosselló-Móra, R. The All-Species Living Tree project: A 16S rRNA-based phylogenetic tree of all sequenced type strains. *Syst. Appl. Microbiol.* **2008**, *31* (4), 241−250.
(44) Hill, M. O. Diversity and Evenness: A Unifying Notation and Its Consequences. *Ecology* **1973**, *54* (2), 427−432.
(45) Jost, L. Entropy and Diversity. *Oikos* **2006**, *113* (2), 363−375.
(46) Jost, L. PARTITIONING DIVERSITY INTO INDEPENDENT ALPHA AND BETA COMPONENTS. *Ecology* **2007**, *88* (10), 2427−2439.
(47) Kang, S.; Rodrigues, J. L. M.; Ng, J. P.; Gentry, T. J. Hill number as a bacterial diversity measure framework with high-throughput sequence data. *Sci. Rep.* **2016**, *6* (1), 38263.
(48) Santini, T. C. Application of the Rietveld refinement method for quantification of mineral concentrations in bauxite residues (alumina refining tailings). *Int. J. Miner. Process.* **2015**, *139*, 1−10.
(49) Hertel, T.; Blanpain, B.; Pontikes, Y. A Proposal for a 100?% Use of Bauxite Residue Towards Inorganic Polymer Mortar. *J. Sustain. Metall.* **2016**, *2* (4), 394−404.
(50) Xue, S.; Zhu, F.; Kong, X.; Wu, C.; Huang, L.; Huang, N.; Hartley, W. A review of the characterization and revegetation of bauxite residues (Red mud). *Environ. Sci. Pollut. Res.* **2016**, *23* (2), 1120−1132.
(51) Ruyters, S.; Mertens, J.; Vassilieva, E.; Dehandschutter, B.; Poffijn, A. Smolders, E. The Red Mud Accident in Ajka (Hungary): Plant Toxicity and Trace Metal Bioavailability in Red Mud Contaminated Soil. *Environ. Sci. Technol.* **2011**, *45* (4), 1616−1622.
(52) Buchman, M. F. *NOAA Screening Quick Reference Tables*; Seattle WA, 2008; Vol. *08−1*.
(53) Barnes, M. C.; Addai-Mensah, J.; Gerson, A. R. The mechanism of the sodalite-to-cancrinite phase transformation in synthetic spent Bayer liquor. *Microporous Mesoporous Mater.* **1999**, *31* (3), 287−302.
(54) Xu, H.; Van Deventer, J. S. J. The geopolymerisation of alumino-silicate minerals. *Int. J. Miner. Process.* **2000**, *59* (3), 247−266.
(55) Langmuir, D. *Aqueous Environmental Geochemistry*; Prentice Hall, 1997.
(56) Wehrli, B.; Stumm, W. Vanadyl in natural waters: Adsorption and hydrolysis promote oxygenation. *Geochim. Cosmochim. Acta* **1989**, *53* (1), 69−77.
(57) Genç, H.; Tjell, J. C.; McConchie, D.; Schuiling, O. Adsorption of arsenate from water using neutralized red mud. *J. Colloid Interface Sci.* **2003**, *264* (2), 327−334.
(58) Sherman, D. M.; Randall, S. R. Surface complexation of arsenic(V) to iron(III) (hydr)oxides: structural mechanism from ab initio molecular geometries and EXAFS spectroscopy. *Geochim. Cosmochim. Acta* **2003**, *67* (22), 4223−4230.
(59) TISDALL, J. M.; OADES, J. M. Organic matter and water-stable aggregates in soils. *J. Soil Sci.* **1982**, *33* (2), 141−163.
(60) Six, J.; Paustian, K.; Elliott, E. T.; Combrink, C. Soil Structure and Organic Matter. *Soil Sci. Soc. Am. J.* **2000**, *64* (2), 681.
(61) Six, J.; Elliott, E. T.; Paustian, K. Soil Structure and Soil Organic Matter. *Soil Sci. Soc. Am. J.* **2000**, *64* (3), 1042.
(62) Knill, C. J.; Kennedy, J. F. Degradation of cellulose under alkaline conditions. *Carbohydr. Polym.* **2003**, *51* (3), 281−300.
(63) Humphreys, P. N.; Laws, A. P.; Dawson, J. *A Review of Cellulose Degradation and the Fate of Degradation Products Under Repository Conditions*; Nuclear Decommissioning Authority (NDA), 2010.
(64) Rout, S. P.; Radford, J.; Laws, A. P.; Sweeney, F.; Elmekawy, A.; Gillie, L. J.; Humphreys, P. N. Biodegradation of the alkaline cellulose degradation products generated during radioactive waste disposal. *PLoS One* **2014**, *9* (9), e107433.
(65) Fuller, R. D.; Nelson, E. D. P.; Richardson, C. J. Reclamation of Red Mud (Bauxite Residues) Using Alkaline-Tolerant Grasses with Organic Amendments1. *J. Environ. Qual.* **1982**, *11* (3), 533.
(66) Wong, J. W. C.; Ho, G. Sewage sludge as organic ameliorant for revegetation of fine bauxite refining residue. *Resour. Conserv. Recycl.* **1994**, *11* (1−4), 297−309.
(67) Krüger, G. Verwitterungsversuche an Leuzit. *Chemie der Erde - Geochemistry1* **1939**, *12*, 236−264.
(68) Brady, P. V.; Walther, J. V. Controls on silicate dissolution rates in neutral and basic pH solutions at 25°C. *Geochim. Cosmochim. Acta* **1989**, *53* (11), 2823−2830.
(69) Hamilton, J. P.; Brantley, S. L.; Pantano, C. G.; Criscenti, L. J.; Kubicki, J. D. Dissolution of nepheline, jadeite and albite glasses: toward better models for aluminosilicate dissolution. *Geochim. Cosmochim. Acta* **2001**, *65* (21), 3683−3702.
(70) Tole, M. P.; Lasaga, A. C.; Pantano, C.; White, W. B. The kinetics of dissolution of nepheline (NaAlSiO4). *Geochim. Cosmochim. Acta* **1986**, *50* (3), 379−392.
(71) Oelkers, E. H. General kinetic description of multioxide silicate mineral and glass dissolution. *Geochim. Cosmochim. Acta* **2001**, *65* (21), 3703−3719.
(72) Álvarez-Ayuso, E.; Nugteren, H. W. Synthesis of Dawsonite: A method to treat the etching waste streams of the aluminium anodising industry. *Water Res.* **2005**, *39* (10), 2096−2104.
(73) Schlesinger, W. H.; Andrews, J. A. Soil respiration and the global carbon cycle. *Biogeochemistry* **2000**, *48* (1), 7−20.
(74) Zhou, J.; Bruns, M. A.; Tiedje, J. M. DNA recovery from soils of diverse composition. *Appl. Environ. Microbiol.* **1996**, *62* (2), 316−322.
(75) Krishna, P.; Babu, A. G.; Reddy, M. S. Bacterial diversity of extremely alkaline bauxite residue site of alumina industrial plant using culturable bacteria and residue 16S rRNA gene clones. *Extremophiles* **2014**, *18* (4), 665−676.
(76) Müller, D. B.; Vogel, C.; Bai, Y.; Vorholt, J. A. The Plant Microbiota: Systems-Level Insights and Perspectives. *Annu. Rev. Genet.* **2016**, *50* (1), 211−234.

DOI: 10.1021/acs.est.7b03568
Environ. Sci. Technol. 2018, 52, 152−161

(77) Bulgarelli, D.; Rott, M.; Schlaeppi, K.; Ver Loren van Themaat, E.; Ahmadinejad, N.; Assenza, F.; Rauf, P.; Huettel, B.; Reinhardt, R.; Schmelzer, E.; et al. Revealing structure and assembly cues for Arabidopsis root-inhabiting bacterial microbiota. *Nature* **2012**, *488* (7409), 91−95.
(78) Lundberg, D. S.; Lebeis, S. L.; Paredes, S. H.; Yourstone, S.; Gehring, J.; Malfatti, S.; Tremblay, J.; Engelbrektson, A.; Kunin, V.; Rio, T. G. del; et al. Defining the core Arabidopsis thaliana root microbiome. *Nature* **2012**, *488* (7409), 86−90.
(79) Jones, R. T.; Robeson, M. S.; Lauber, C. L.; Hamady, M.; Knight, R.; Fierer, N. A comprehensive survey of soil acidobacterial diversity using pyrosequencing and clone library analyses. *ISME J.* **2009**, *3* (4), 442−453.
(80) Liu, W.; Zhang, W.; Liu, G.; Zhang, Y.; Zhang, G. Microbial diversity in the saline-alkali soil of a coastal Tamarix chinensis woodland at Bohai Bay, China. *J. Arid Land* **2016**, *8* (2), 284−292.
(81) Huber, K. J.; Geppert, A. M.; Wanner, G.; Fösel, B. U.; Wüst, P. K.; Overmann, J. The first representative of the globally widespread subdivision 6 Acidobacteria,Vicinamibacter silvestris gen. nov., sp. nov., isolated from subtropical savannah soil. *Int. J. Syst. Evol. Microbiol.* **2016**, *66* (8), 2971−2979.
(82) Li, X.; Sun, M.; Zhang, H.; Xu, N.; Sun, G. Use of mulberry−soybean intercropping in salt−alkali soil impacts the diversity of the soil bacterial community. *Microb. Biotechnol.* **2016**, *9* (3), 293−304.
(83) Lage, O. M.; Bondoso, J. Bringing Planctomycetes into pure culture. *Front. Microbiol.* **2012**, *3*, 405.
(84) Chistoserdova, L.; Jenkins, C.; Kalyuzhnaya, M. G.; Marx, C. J.; Lapidus, A.; Vorholt, J. A.; Staley, J. T.; Lidstrom, M. E. The Enigmatic Planctomycetes May Hold a Key to the Origins of Methanogenesis and Methylotrophy. *Mol. Biol. Evol.* **2004**, *21* (7), 1234−1241.
(85) Scheuner, C.; Tindall, B. J.; Lu, M.; Nolan, M.; Lapidus, A.; Cheng, J.-F.; Goodwin, L.; Pitluck, S.; Huntemann, M.; Liolios, K.; et al. Complete genome sequence of Planctomyces brasiliensis type strain (DSM 5305T), phylogenomic analysis and reclassification of Planctomycetes including the descriptions of Gimesia gen. nov., Planctopirus gen. nov. and Rubinisphaera gen. nov. and emended descriptions of the order Planctomycetales and the family Planctomycetaceae. *Stand. Genomic Sci.* **2014**, *9* (1), 10.
(86) Ferreira, C.; Soares, A. R.; Lamosa, P.; Santos, M. A.; da Costa, M. S. Comparison of the compatible solute pool of two slightly halophilic planctomycetes species, Gimesia maris and Rubinisphaera brasiliensis. *Extremophiles* **2016**, *20* (6), 811−820.
(87) Elshahed, M. S.; Youssef, N. H.; Luo, Q.; Najar, F. Z.; Roe, B. A.; Sisk, T. M.; Bühring, S. I.; Hinrichs, K.-U.; Krumholz, L. R. Phylogenetic and metabolic diversity of Planctomycetes from anaerobic, sulfide- and sulfur-rich Zodletone Spring, Oklahoma. *Appl. Environ. Microbiol.* **2007**, *73* (15), 4707−4716.

DOI: 10.1021/acs.est.7b03568
Environ. Sci. Technol. 2018, 52, 152−161